A common subcortical oscillatory network contributes to recovery after spinal cord injury

Yukio Nishimura[1, 2, *] Yosuke Morichika[1] & Tadashi Isa[1, 2, 3]

[1]Department of Developmental Physiology, National Institute for Physiological Sciences, Okazaki, Japan
[2] Core Research for Evolutional Science and Technology, Japan Science and Technology Agency, Kawaguchi, Japan
[3] Graduate University for Advanced Studies (SOKENDAI), Hayama, Japan

Present address; Box 357330 Department of Physiology and Biophysics and Washington National Primate Research Center, University of Washington, Seattle, Washington, USA

Corresponding should be addressed to Yukio Nishimura yukio@u.washington.edu or Tadashi Isa tisa@nips.ac.jp

Abstract: 152 words
Main text: 2,640 words
Methods and Authors contribution: 1,119 words
References: 931 words
Figure: 6 figures

Abstract

Recent studies in monkeys showed that when the direct cortico-motoneuronal connection was transected at mid-cervical segments, remaining, indirect cortico-motoneuronal pathways compensated for finger dexterity within one to three months. To elucidate the changes in dynamic properties of neural circuits during the recovery, we investigated the cortico-muscular and inter-muscular couplings of activities throughout the recovery course. Activities of antagonist muscle pairs showed co-activation during the second postoperative week, and oscillated coherently at frequencies of 30-46 Hz (γ–band) by one month postoperatively. Such γ–band inter-muscular coherence was not observed preoperatively, but became prominent and distributed widely over proximal and distal muscles with the recovery. Neither the β-band cortico-muscular coupling (14-30 Hz) observed before lesion, nor a γ–band oscillation was observed in bilateral motor cortex after lesion. Thus, we propose that an unknown, subcortical oscillator, independent of cortical oscillation, commonly recruits hand/arm muscles and may underlie functional recovery of dexterous finger movements.

Understanding the neural mechanisms of functional recovery after partial lesion of the central nervous system will contribute to establishing a roadmap of neuro-rehabilitational therapy for patients with brain damage or spinal cord injury. The macaque monkey models of brain/spinal cord injury are valuable because the structures of the macaque CNS and motor apparatus are similar to those of human[1]. In these monkeys, the dexterity of finger movements, such as precision grip and independency of individual fingers, recovers within one to three months after lesion of the lateral corticospinal tract (l-CST) at the C4/C5 cervical spinal segments[2,3]. Based on this finding, it was postulated that functions of the direct cortico-motoneuronal (CM) pathway might be taken over by remaining neuronal pathways, presumably mediated by propriospinal and/or reticulospinal neurons[2-6]. We have been using this animal model to clarify the neural mechanisms of functional compensation after spinal cord injury. In a recent study, we investigated the role of cortical motor-related regions and found that recovery is based on increased activity in the bilateral primary motor cortex (M1) at the early stage (around one month postoperatively) and an expanded area of activation in the contralateral M1 and bilateral ventral premotor cortex (PMv) at later stages of recovery (after three months postoperatively)[3]. In the present study, to characterize changes in the dynamic properties of neural networks connecting the motor cortices and

hand/arm muscles, we simultaneously recorded local field potentials (LFPs) in bilateral M1 and electromyography (EMG) of various hand/arm muscles in two monkeys, and analyzed the cortico-muscular and inter-muscular couplings during a force tracking, precision grip task both before spinal cord lesion and during the recovery course.

Results

Extent of the spinal cord lesion

Fig. 1A shows the extents of the spinal cord lesions at the C4/C5 border in the two monkeys. Fig. 1Ab and 1Ac indicates the normal distribution of the l-CST in sections rostral (C3, Fig. 1Ab) and caudal (C6, Fig. 1Ac) to the lesion, revealed by CaMKII immunohistochemistry. Lesions in both monkeys appeared to encompass the normal distribution of the l-CST (compare the blackened areas in Fig. 1Aa with the areas where labeled axons are distributed in Fig. 1Ab on both sides and in Fig. 1Ac only on the right side). CaMKII immunohistochemistry demonstrated robust staining of immunopositive axons rostral to lesion on both sides (C3, Fig. 1Ab), while no CaMKII -positive axons caudal to lesion on the lesioned side (C6, Fig. 1Ac). Thus, lesion of the l-CST was regarded as complete in both monkeys.

Recovery of finger dexterity

Independent control of digits and performance of precision grip showed deficits one day after the lesion. In both monkeys, the success ratio of precision grip dropped to zero on the first day; however, performances gradually recovered and success ratios reached nearly 100% approximately five to seven weeks after the lesions (Fig. 1B) as shown in previous studies[2,3].

Cortico-muscular coupling

LFPs in bilateral M1 hand area and EMGs in various hand/arm muscles were simultaneously recorded preoperatively during a force tracking precision grip task (Fig. 2). In Monkey Mu, Fourier analysis revealed that the LFPs in the hand area of bilateral M1 included peaks of power at both α- (8-13 Hz) and β- (14–30 Hz) frequency bands (Fig. 3Aa, d). The peak at the β-band was higher than that at the α-band in both hemispheres. During this time, the EMG activity of an intrinsic hand muscle (ADP: *adductor pollicis*) contained frequency components over a broad range (Fig. 3Ag). Coherence analysis of the LFP and the EMG showed clear cortico-muscular coupling (CMC) between the contralateral M1 and ADP at the β-band with a peak at 17 Hz (Fig. 3Ab, c), whereas no coherency was found between the ipsilateral M1 and ADP (Fig. 3Ae, f). During the first month after the l-CST lesion, the β-band oscillatory component

of the LFP in M1 decreased, and the α–band component predominated instead (Fig. 3Ba, Ca). But by postoperative day 92, the β-band oscillation recovered (Fig. 3Da, d) on both sides. The EMG activities of ADP started showing oscillatory activity around 33 Hz which is in the γ-band range during recovery (Fig. 3 Cg, Dg); however, the cortico-muscular coupling disappeared completely and had not recovered at all by postoperative day 92 (Fig. 3Bb, Cb, Db), when the ability of precision grip already recovered (Fig.1B). By comparison, in Monkey Be, although the M1 LFP showed oscillations at both the α– and β-bands, no coupling was observed between LFP and EMG activity before the lesion, as previously reported in some healthy human subjects[7,8], or during the recovery (data not shown).

Inter-muscular coupling

We then analyzed the activation patterns of various arm/hand muscles during the force tracking precision grip task. Figure 4 shows the EMG activity of ADP, a primary mover of the precision grip, and ED23, an antagonist of the ADP in Monkey Be. Preoperatively, ED23 was activated just before the grip and ADP was activated during the grip. Thus, these muscles showed reciprocal activation (Fig. 4Aa) and as a consequence, long-term synchrony (co-activation) was not observed, as evidenced by

the absence of a positive correlation peak at the zero lag time in the cross-correlogram (Fig. 4Ab). However, on postoperative day 14, these two muscles started showing co-activation (Fig. 4Ba), which resulted in the appearance of a positive broad correlation peak at the zero lag time (Fig. 4Bb). The co-activation became more evident on postoperative day 34 (Fig. 4Ca), as evidenced by an increase in the positive correlation peak at the zero lag time (Fig. 4Cb). On postoperative day 92, the positive correlation peak was slightly smaller, but still prominent (Fig. 4Db). These results indicate that muscle pairs that were antagonistic preoperatively became agonistic, developing long-term synchrony during the recovery from l-CST lesion. Correlation coefficients between each muscle pair at the zero lag time, indicated with the vertical gray line in individual cross-correlograms, were plotted in Figures 4E and F. These indicate long-term synchrony of the ED23 (Fig. 4Ea and 4Fa) and ADP (Fig. 4Eb and Fb) muscles with other hand/arm muscles, respectively, during the recovery course. Preoperatively, these correlation coefficients of muscle pairs varied considerably from negative to positive values. In monkey Be, most of the correlation coefficients increased during the first month, and then those of some pairs increased or decreased slightly later (Fig. 4Ea, b). In Monkey Mu, most correlation coefficients between muscles paired with ED23 and with ADP increased during the first or second postoperative month,

respectively, but decreased slightly later (Fig. 4Fa, b). Correlation coefficients between all muscle pairs were positive at one time after lesion in both monkeys. Thus, the co-activation pattern of antagonist muscles was widespread among various muscle pairs over both proximal and distal joints of the upper extremity.

In addition to the postoperative emergence of long-term synchrony, the EMG activities of muscles ADP and ED23 also became oscillatory and coherent. Prior to spinal cord lesions, the EMG activity of the ED23 muscle contained frequency components over a broad range (Fig. 5Ab), and that of the ADP had some small peaks at specific frequencies (Fig. 5Ac) of the power spectra, but there was no peak for coherence above the β frequency (Fig. 5Ad, e). By postoperative day 14, however, both ADP and ED23 started showing oscillatory activity around 30 Hz (Fig. 5Ba, b, c), although there was no coherence between them at this stage (Fig. 5Bd, e). But on postoperative day 34-92, the 30 Hz oscillatory activities of these muscles were coupled (Fig. 5C, D), and the coherence between them increased further (Fig. 5Cd, e and 5Dd, e). Such inter-muscular coupling (IMC) was widespread, occurring among a variety of hand/arm muscles, and not only between synergistic muscle pairs but also between antagonistic muscle pairs and between muscle pairs of various joints, including distal and proximal ones (Fig. 5E and F). The peak frequency of coherence was detected at

33.24 ± 0.34 Hz (mean ± S.D.; range 30–46 Hz). In Monkey Be, the coupling between most muscle pairs continuously increased through postoperative day 92, and decreased in only two pairs (Fig. 5Ea, b). In Monkey Mu, by contrast, the coupling between most muscle pairs increased sometime during the first postoperative one to two months, but then decreased during the third month. Only the coupling between the ADP and ED23 muscles maintained a high degree of coherency throughout the recovery (Fig. 5Fa, b). Such γ-band oscillatory LFP activities and coherence with muscle activities were not found in either the contra- or ipsilesional M1 (see Fig. 3B-D a, b and d, e), or the contralesional PMv or somatosensory (S1) cortices (data not shown). Cortical activity displayed oscillatory components at either the α-band (8-13 Hz) or β–band (14-30 Hz) frequencies; both lower than 30 Hz. Therefore, the IMC at frequencies of 30-46 Hz, which emerged during the course of recovery, was probably independent of cortical oscillation.

Discussion

In a previous study, we demonstrated a time-dependent change in activation of cortical networks during the functional recovery of finger dexterity after lesion of the l-CST[3]. However, because we employed brain imaging and reversible inactivation

techniques, both of which have low temporal resolutions, actual changes in the dynamic properties of the neural circuits were not visible. In the present study we used electrophysiological analyses to clarify the change in dynamic properties of the neural networks connecting the motor-related cortices and hand/arm muscles. Cross-correlation and coherence analyses of EMG and cortical LFPs provide valuable information on the organization of networks responsible for driving spinal motoneurons during voluntary movement[9-12].

Previous studies showed that oscillations in the motor cortex of monkeys and humans are dominated by activity in the frequency range of 15-30 Hz[7, 8, 11, 13-19]. Moreover, coherence was detected between cortical and muscle activities with a peak at 15-30 Hz in humans using electro- and magnetoencephalography and in monkeys using LFP recordings, especially during the hold phase of tasks[7, 8, 11, 17, 18, 20-23]. It was proposed that such cortico-muscular coupling is mediated by the monosynaptic CM pathway, which has a particularly pronounced influence over distal limb function[9,10]. In support of this assumption, phase lags between cortex and muscle were consistent with conduction over the fast corticospinal pathway[22,23], and additionally, the coupling was reduced in patients with internal capsule lesions[24,25]. However, in those studies, it was not clear whether the direct CM connection was required for generating the coherence,

or the coherence could be mediated by indirect CM pathways via subcortical or spinal interneuronal systems, because in the patients with internal capsule lesions, most of the indirect CM pathways, mediated via those interneurons, were also damaged. The present study demonstrated that after lesions of the l-CST at the C4/C5 segments, cortico-muscular coupling did not recover, even though the monkeys showed prominent recovery of precision grip, and β-band oscillation recovered in the cortical LFP (Fig. 3D). A large proportion of indirect CM pathways, except for those mediated by segmental interneurons, remained intact in the present preparation[2,3,6]. Therefore, the results suggest that recovery of finger dexterity is not related to β–band cortico-muscular coupling. On the other hand, the present results also suggest that the direct CM connection is necessary for generation of the coherence as previously proposed[22-27]. However, it was also proposed that feedback from peripheral afferents is involved in generating the β–band cortico-muscular coupling [28, 29]. Therefore, the possibility cannot be excluded that disappearance of this coupling after the l-CST lesion was due to interruption of the sensory-motor loop between the periphery and spinal motoneurons via motor cortices, or loss of the cortical control of sensory feedback at the level of the lower cervical spinal cord.

Even preoperatively, Monkey Be did not display CMC at any frequency band.

This is not surprising, as previous studies reported that such coupling was significantly smaller when the task was performed under an isometric condition than under a compliant condition in which subjects moved the levers against a spring-like load;[7] moreover, some healthy human subjects do not exhibit such coupling even under compliant conditions[8].

During the recovery period, both monkeys showed marked changes in the motor strategy for precision grip. Apparently, they could control their fingers independently and became successful in precision grip with just the index finger and thumb, while other fingers were kept flexed, as previously reported[2, 3]. However, as the recovery progressed, preoperatively antagonist muscles started working as agonists, showing long-term synchrony indicative of co-activation of a variety of forearm muscles, from proximal to distal. Such a strategy to increase stiffness might play a role during the learning of novel motor strategies in intact subjects[30].

Surprisingly, as the recovery progressed, the coupling between pairs of a variety of hand/arm muscles increased, with a coherence peak at 30-46 Hz, which corresponds to the γ-band. This was a robust finding, observed in both Monkey Be and Mu. In addition, although not reported in this study, we observed IMC in another monkey (Monkey S in a previous report[3]) later than three months postoperatively during

a reaching and grasping task that did not include a static phase as in the present experiments. The β-band coherence (15-30 Hz) of EMG activity between pairs of muscles was reported previously and thought to originate from the cerebral cortex[9, 10, 12, 21]. This assumption derived from the observation that β-band coherence between muscle pairs was reduced in patients with internal capsule lesions[10] and spinal cord injury[12], suggesting that pyramidal tract activity is involved in its generation. The 24-40 Hz IMC in antagonist muscle pairs has not been shown in normal subjects, but was observed in patients with incomplete injury of the CST[31]. This finding is similar to that of the present study, but the authors' interpretation of how the coupling emerges is different. They suggested that, because the coherence value for the coupling was correlated with the amplitude of corticospinal conduction (assessed from motor evoked potential in response to transcranial magnetic stimulation) the 24-40 Hz coupling represented an increase in a common corticospinal drive to the antagonist muscle pair[31, 32]. However, the frequency of such a 24-40 Hz IMC in patients with spinal cord injury appears to be higher than either the classical β-beta band CMC[17-23] or cortical oscillation[13-19]. The present study demonstrates that the γ-band (30-46 Hz) IMC in both agonist and antagonist muscle pairs was generated in monkeys in which the direct CM connection was completely transected. Moreover, the coherence increased along with the functional

recovery. In addition, after the recovery, the preoperatively recorded cortical oscillation at around 17 Hz was not coupled with EMG activity. This was the case not only for the contralateral M1, but also for the ipsilateral M1, and the contralateral PMv and S1. Based on these findings, as shown in Figure 6, we propose that the γ-band IMC, which emerges during recovery, represents an increasing common drive from subcortical neuronal systems and/or peripheral afferents to various spinal motoneuron pools. The neuronal substrate of such a "common subcortical oscillator" is not clear at this moment. The interneuronal systems mediating indirect CM drive and/or reflex afferents from the periphery, which remained after the lesion, may possibly contribute to its generation. Because the coherence appears only when movements are voluntarily driven, the common subcortical oscillator might also be driven by descending inputs from the cerebral cortex and/or by peripheral feedback associated with the movement. They might include, 1) propriospinal neurons with cell bodies in the C3-C4 segments and with axons passing through the ventral part of the lateral funiculus toward hand/arm muscle motoneurons[4,5], 2) reticulospinal neurons that control both proximal and distal hand/arm muscles[33,34], 3) the subcortical reflex pathways through the brainstem or spinal cord.

It is not clear whether the γ-band IMC observed during the recovery is physiological

or pathological at this stage. However, a challenging hypothesis is that oscillation and coherence provide a beneficial means for the limited neuronal resources available after the l-CST lesion to effectively compensate for the motor ability.

Methods

Subjects

Two monkeys **(***Macaca mulatta***,** Monkey B**e**: male 9.1 kg, Monkey Mu: male 5.7 kg were used in the present study. The experimental procedures were subjected to prior reviews by the ethical committee of the National Institute of Natural Science and were performed in accordance with the NIH Guideline for the Care and Use of Laboratory Animals.

Surgeries

All surgeries were performed under general deep anesthesia, starting with a combination of ketamine (10 mg/kg, i.m.) and xylazine (1 mg/kg, i.m.) and followed by sodium pentobarbital (25 mg/kg, i.v.). Supplemental doses of ketamine (5 mg/kg with saline, i.v.) were given as needed during surgery. Diclofenac sodium (Voltaren, Novartis, Tokyo) was routinely applied to the anus for analgesia after surgery.

Spinal cord injury

A full description of the method for transecting the l-CST has been published previously[2,3]. Briefly, the border between the C4 and C5 spinal cord segments was exposed by laminectomy of the C3 and C4 vertebrae, and a transverse opening was made in the *dura mater*. The l-CST lesion was made under a surgical microscope using forceps. The dorsal part of the lateral funiculus was transected from the dorsal root entry zone ventrally to the convexity of the spinal cord. Then the lesion was extended ventrally at the most lateral part of the lateral funiculus. The opening of the *dura mater* was closed, and the skin and back muscles were sutured with nylon or silk. Both monkeys received the l-CST lesion on left side.

Surgery for LFP recording

The skull over the bilateral frontal cortices was widely exposed for recording LFPs in bilateral M1, PMv and S1. After partial removal of the skull, the cortex around the precentral gyrus was exposed bilaterally, and a chamber was attached to cover the opening on the right hemisphere (contralateral to the lesion). Movable implantable electrodes were chronically implanted in the digit area of the primary motor cortex on

the left hemisphere (ipsilateral to the lesion). Small titanium-steel screws were attached to the skull as anchors. Two stainless-steel tubes were mounted in parallel over the frontal and occipital lobes for head fixation. The chamber and stainless steel tubes were fixed to the screws with acrylic resin.

Surgery for EMG recording

EMG activities from muscles of the forelimb on left side were recorded from implanted pairs of multi-stranded, stainless steel wires (Cooner Wire, Chatsworth, CA, US), subcutaneously tunneled to their target muscles. Circular connectors (MCP-12, Omnetics, Minneapolis, MN, US) were anchored to the skull.

Behavioral test for evaluation of functional recovery

To assess functional recovery of dexterous finger movements before and after transection of the l-CST, the monkeys were trained to reach, grasp, and retrieve a small piece of sweet potato (about 7 mm^3) through a narrow vertical slit using both the index finger and thumb. The food piece was positioned in the center of vertical slit, and the success ratio of food retrieval from the pin was evaluated as finger dexterity. A success trial was defined as any trial that resulted in the successful precision grip and removal of

the food from the pin without dropping it. Each experiment consisted of 30 trials.

Behavioral task for recording

Monkeys were trained to do the force tracking precision grip task (Fig. 2) for juice reward with left hand which is ipsilateral side to the lesion. The task required that two independent levers be pinched between the index finger and the thumb and held within their respective, electronically defined isometric force windows. Both levers had to be held correctly for 3.5 s, after which a tone signaled that the levers could be released to obtain a reward.

Data collection

We recoded LFPs from a glass-coated Elgiloy electrode (0.9-1.4 MΩ at 1 kHz) in the contralesional hemisphere and chronically implanted electrodes (Polyurethane-coated tungsten electrode, 0.8-1.2 MΩ at 1 kHz, Unique Medical, Osaka, Japan) in the ipsilesional hemisphere. Following preamplification, the signals from each electrode were filtered at 5-500 Hz. EMGs were recorded from selected forearm muscles. In monkey Be, EMGs were recorded from two *intrinsic hand muscles*: adductor pollicis (ADP) and first dorsal interosseus (FDI); four *digit muscles*: extensor

digitorum communis (EDC), extensor digitorum 2 and 3 (ED23), extensor digitorum 4 and 5 (ED45), and flexor digitorum superficialis (FDS); three *wrist muscles*: flexor carpi radialis (FCR), flexor carpi ulnaris (FCU), and palmaris longus (PL); and one *elbow muscle*: biceps brachii (BB). In monkey Mu, EMGs were recorded from two *intrinsic hand muscles*: ADP and FDI; three *digit muscles*: EDC, ED23, FDS; two *wrist muscles*: FCU, and extensor carpi ulnaris (ECU); and one *elbow muscle*: BB. EMG signals were amplified, filtered (5 Hz-3 kHz), and rectified. All signals (LFPs, EMGs, and finger forces) were sampled at 4 kHz and recorded through a 1401 A-D converter (Cambridge Electronic Design, Cambridge, UK) onto a computer using Spike2 software (Cambridge Electronic Design, Cambridge, UK).

Analysis of functional coupling

For coherence and cross-correlation analyses of LFP and EMG signals, a Spike2 software script was employed. Coherence and cross-correlation estimates for CMC and IMC (Figures 3 and 5) were calculated during the hold phase of force production. Coherence and power spectra were calculated using non-overlapping segments that were 2,048 samples long (240 epochs). Cross-correlation estimates of long-term synchronization in Figure 4 were calculated from 0.5 s before the increase of

thumb force to the end of force production. The penetration track with the highest LFP-EMG coherence was selected for further analyses. We excluded records from muscle pairs demonstrating cross-talk between the EMG records as evidenced by high, narrow peaks in the cross-correlogram at the zero lag time and a high degree of coherence at all frequencies.

Histological assessment of lesion completeness

At the end of the experiments, the monkeys were deeply anesthetized with an overdose of sodium pentobarbital (> 70 mg/kg) and transcardially perfused with 4% paraformaldehyde in 0.1 M phosphate buffered saline pH7.3 (PBS). The spinal cords were removed immediately, saturated with 30% sucrose in 0.1 M PBS (pH 7.3), and then cut serially into 50-μm-thick coronal sections on a freezing microtome. The sections were either processed with Klüver-Barrera Nissl-staining with 1% Cresyl Violet or immunostained with anti-calmodulin-dependent protein kinase IIα (CaMKIIα) antibody (Affinity BioReagents, Golden, CO, US) according to the manufacturer's instructions to examine the remaining CST.

Acknowledgements

Supported by grants from the Core Research for Evolutional Science and Technology (CREST), Japan Science and Technology Agency (JST), and from the Ministry of Education, Culture, Sports, Science and Technology of Japan (the grant for higher priority area –the Integrative Brain Research- project No. 18200027). We thank Masahiro Mori and Kaoru Isa for technical assistance and Junichi Ushiba for assistance in experimental setup.

Author contributions

Y.N. planned the experiment with T.I. Y.N. performed the experiment with Y.M. Y.N. and T.I. wrote the manuscript.

References

1.Courtine G, Bunge MB, Fawcett JW, Grossman RG, Kaas JH, Lemon R, Maier I, Martin J, Nudo RJ, Ramon-Cueto A, Rouiller EM, Schnell L, Wannier T, Schwab ME, Edgerton VR. Can experiments in nonhuman primates expedite the translation of treatments for spinal cord injury in humans? *Nat Med*. 13:561-566. (2007)

2. Sasaki S, Isa T, Pettersson LG, Alstermark B, Naito K, Yoshimura K, Seki K, Ohki Y. Dexterous finger movements in primate without monosynaptic corticomotoneuronal excitation. *J Neurophysiol.* 92:3142-3147. (2004)

3. Nishimura Y, Onoe H, Morichika Y, Perfiliev S, Tsukada H, Isa T. Time-dependent central compensatory mechanisms of finger dexterity after spinal cord injury. *Science.* 318:1150-1155. (2007)

4. Alstermark B, Isa T, Ohki Y, Saito Y. Disynaptic pyramidal excitation in forelimb motoneurons mediated via C3-C4 propriospinal neurons in the Macaca fuscata. *J. Neurophysiol.* 82:3580-3585. (1999)

5. Isa T, Ohki Y, Seki K, Alstermark B. Properties of propriospinal neurons in the C3-C4 segments mediating disynaptic pyramidal excitation to forelimb motoneurons in the macaque monkey. *J Neurophysiol.* 95:3674-3685 (2006)

6. Isa T, Ohki Y, Alstermark B, Pettersson L-G, Sasaki S. Direct and indirect

cortico-motoneuronal pathways and control of hand/arm movements. *Physiology* (Bethesda). 145-152. (2007)

7. Kilner JM, Baker SN, Salenius S, Hari R, Lemon RN. Human cortical muscle coherence is directly related to specific motor parameters. *J. Neurosci.* 20:8838-8845. (2000)

8. Baker MR and Baker SN. The effect of diazepam on motor cortical oscillations and corticomuscular coherence studies in man. *J Physiol.(Lond)*, 546.3 931-942 (2003)

9. Farmer SF, Bremner FD, Halliday DM, Rosenberg JR, Stephens JA. The frequency content of common synaptic inputs to motoneurones studied during voluntary isometric contraction in man. *J Physiol. (Lond)* 470:127-155. (1993)

10. Farmer SF, Swash M, Ingram DA, Stephens JA. Changes in motor unit synchronization following central nervous lesions in man. *J Physiol. (Lond)* 463:83-105. (1993)

11. Halliday DM, Conway BA, Farmer SF, Rosenberg JR. Using electroencephalography to study functional coupling between cortical activity and electromyograms during voluntary contractions in humans. *Neurosci Lett.* 241:5-8 (1998)

12. Hansen NL, Conway BA, Halliday DM, Hansen S, Pyndt HS, Biering-Sorensen F,

Nielsen JB. Reduction of common synaptic drive to ankle dorsiflexor motoneurons during walking in patients with spinal cord lesion. *J Neurophysiol.* 94:934-942. (2005)

13. Murthy VN, Fetz EE. Coherent 25- to 35-Hz oscillations in the sensorimotor cortex of awake behaving monkeys. *Proc Natl Acad Sci U S A.* 89:5670-5674. (1992)

14. Murthy VN, Fetz EE. Oscillatory activity in sensorimotor cortex of awake monkeys: synchronization of local field potentials and relation to behavior. *J Neurophysiol.* 76:3949-3967. (1996)

15. Murthy VN, Fetz EE. Synchronization of neurons during local field potential oscillations in sensorimotor cortex of awake monkeys. *J Neurophysiol.* 76:3968-3982. (1996)

16. Sanes JN, Donoghue JP. Oscillations in local field potentials of the primate motor cortex during voluntary movement. *Proc Natl Acad Sci U S A.* 90:4470-4474 (1993)

17. Conway BA, Halliday DM, Farmer SF, Shahani U, Maas P, Weir AI, Rosenberg JR. Synchronization between motor cortex and spinal motoneuronal pool during the performance of a maintained motor task in man. *J Physiol. (Lond)* 489:917-924. (1995)

18. Baker SN, Olivier E, Lemon RN. Coherent oscillations in monkey motor cortex and hand muscle EMG show task-dependent modulation. *J Physiol. (Lond)* 501:225-241. (1997)

19. Hari R, Salenius S. Rhythmical corticomotor communication. *Neuroreport.* 10:1-10. (1999)

20. Salenius S, Portin K, Kajola M, Salmelin R, Hari R. Cortical control of human motoneuron firing during isometric contraction. *J Neurophysiol*. 77:3401-3405. (1997)

21. Kilner JM, Baker SN, Salenius S, Jousmaki V, Hari R, Lemon RN. Task-dependent modulation of 15-30 Hz coherence between rectified EMGs from human hand and forearm muscles. *J Physiol. (Lond)* 516 :559-570. (1999)

22. Gross J, Tass PA, Salenius S, Hari R, Freund HJ, Schnitzler A. Cortico-muscular synchronization during isometric muscle contraction in humans as revealed by magnetoencephalography. *J Physiol. (Lond)* 527:623-631. (2000)

23. Mima T, Steger J, Schulman AE, Gerloff C, Hallett M. Electroencephalographic measurement of motor cortex control of muscle activity in humans. *Clin Neurophysiol.* 111:326-337. (2000)

24. Mima T, Toma K, Koshy B, Hallett M. Coherence between cortical and muscular activities after subcortical stroke. *Stroke.* 32:2597-2601. (2001)

25. Braun C, Staudt M, Schmitt C, Preissl H, Birbaumer N, Gerloff C. Crossed cortico-spinal motor control after capsular stroke. *Eur J Neurosci.* 25:2935-2945 (2007)

26. Jackson A, Spinks RL, Freeman TC, Wolpert DM, Lemon RN. Rhythm generation

in monkey motor cortex explored using pyramidal tract stimulation. *J Physiol. (Lond)* 541:685-699. (2002)

27. Hansen NL, Nielsen JB. The effect of transcranial magnetic stimulation and peripheral nerve stimulation on corticomuscular coherence in humans. *J Physiol. (Lond)* 561:295-306. (2004)

28. Riddle CN, Baker SN. Manipulation of peripheral neural feedback loops alters human corticomuscular coherence. *J Physiol. (Lond)* 566: 625-639. (2005)

29. Baker SN, Chie M, Fetz EE. Afferent encoding of central oscillations in the monkey arm. *J Neurophysiol.* 95; 3904-3910. (2006)

30. Osu R, Franklin DW, Kato H, Gomi H, Domen K, Yoshioka T, Kawato M. Short- and long-term changes in joint co-contraction associated with motor learning as revealed from surface EMG. *J Neurophysiol.* 88:991-1004. (2002)

31. Norton JA, Gorassini MA. Changes in cortically related intermuscular coherence accompanying improvements in locomotor skills in incomplete spinal cord injury. *J Neurophysiol.* 95:2580-2589 (2006)

32. Thomas SL, Gorassini MA. Increases in corticospinal tract function by treadmill training after incomplete spinal cord injury. *J Neurophysiol.* 94:2844-2855. (2005)

33. Davidson AG, Schieber MH, Buford JA. Bilateral spike-triggered average effects in

arm and shoulder muscles from the monkey pontomedullary reticular formation. *J Neurosci*. 27:8053-8058.

34. Davidson AG, Buford JA. Bilateral actions of the reticulospinal tract on arm and shoulder muscles in the monkey: stimulus triggered averaging. *Exp Brain Res.* 173:25-39. (2006)

Figure legends

Figure 1. Extent of spinal cord lesion (**A**) and recovery of hand dexterity (**B**). **Aa**: Drawings of the C4/C5 segments showing the extent of the l-CST lesion (labeled in black) in two monkeys. **Ab**: CaMKII staining of spinal sections rostral to the lesion site (C3). **Ac**: CaMKII staining of spinal sections caudal to the lesion site (C6). Because CaMKII is known to be transported in CST axons, absence of labeled axons caudal to the lesion site indicates a complete lesion of unilateral l-CST. **B**: Recovery time course of hand dexterity in two monkeys. Performance of precision grip was plotted against the time after lesion.

Figure 2. An example of unprocessed recordings of local field potentials (LFPs) from primary motor cortex in both hemispheres and rectified EMGs in a variety of forearm muscles in ipsilesional side, together with the force applied to the levers by the index finger and thumb during the force tracking precision grip task. Note that oscillatory activity in the LFP appears in both hemispheres during the hold phase. Data was obtained in Monkey Mu before lesion. Abbr.: coM1; primary motor cortex in the contralesional hemisphere, ipM1; primary motor cortex in the ipsilesional hemisphere, BB; *biceps brachii*, EDC; *extensor digitorum communis*, FDS; *flexor digitorum*, ED23; *extensor digitorum*, ADP; *adductor pollicis*.

Figure 3. Cortico-muscular coupling recorded at various times before and after the l-CST lesion. **A**: preoperatively, **B**: postoperative day 14, **C**: postoperative day 33, postoperative day 92. **a**: Power spectra of LFP in contralesional M1. **b**: coherence between LFP in contralesional M1 and EMG of ADP in ipsilesional side. **c**: cross-correlogram between LFP in contralesional M1 and EMG of ADP in ipsilesional

side. **d**: Power spectra of LFP in ipsilesional M1. **e**: coherence between LFP in ipsilesional M1 and EMG of ADP in ipsilesional side. **f**: cross-correlogram between LFP in ipsilesional M1 and EMG of ADP in ipsilesional side. **g**: Power spectra of EMG of ADP in ipsilesional side. Coherence and cross-correlation estimates in this figure were calculated during the hold phase of force production. In the coherence plots of a and d, the gray horizontal lines represent the 95% confidence limit of 0.0125. The vertical gray lines in the cross-correlograms represent the zero lag time. Data in this figure were obtained in Monkey Mu.

Figure 4. Long-term synchronization of muscle pairs (ED23 and ADP) recorded at various times before and after the l-CST lesion. Data were obtained from 0.5 s before the increase of force in the thumb to the end of force production. **A-D**: From preoperatively (**A**), postoperative day 14 (**B**), postoperative day 33 (**C**), and postoperative day 92 (**D**). **a**: the EMG activity from ED23 (*top*) and ADP (*middle*), and force trajectory of thumb (*bottom*). **b**: Cross-correlograms between ED23 and ADP. The gray vertical lines represent zero lag time in the cross-correlograms. These data were obtained from Monkey Be. **E, F**: Changes in long-term synchronization of muscle pairs during recovery in Monkey Be (**E**) and Monkey Mu (**F**). Correlation coefficients of the activities of muscle pairs at zero lag time, indicated with vertical gray lines in each cross-correlograms, are plotted. **a**: Correlations between ED23 activity and that of a variety of other muscles (see inset). **b**: Correlations between ADP activity and that of a variety of other muscles (see inset). Abbreviations; ADP: *adductor pollicis*, FDI: first dorsal interosseus, EDC: extensor *digitorum communis*, ED23: *extensor digitorum 2 and 3*, ED45: *extensor digitorum 4 and 5*, FDS: *flexor digitorum superficialis*, FCR: *flexor*

carpi radialis, FCU: *flexor carpi ulnaris*, PL: *palmaris longus*, ECU: *extensor carpi ulnaris*, BB: *biceps brachii*

Figure 5. Oscillatory coupling of muscle pair (ED23 and ADP) activities recorded at various times before and after the l-CST lesion. **A-D**: preoperatively (**A**), postoperative day 14 (**B**), postoperative day 34 (**C**), and postoperative day 92 (**D**). **a**: the rectified EMG activity from ED23 (*top*) and ADP (*bottom*). Data obtained during the hold phase of precision grip in Monkey Be. **b** and **c**: power spectra of ED23 and ADP, respectively. **d**: coherence between ED23 and ADP. In the coherence plots, the gray horizontal lines represent the 95% confidence limit (0.0125). **e**: Cross-correlograms between ED23 and ADP. In cross-correlograms, the y-axes on the right and left sides indicate the absolute and relative values, respectively. The gray vertical lines in the cross-correlograms represent the zero lag time. **E,F**: Changes in the 30-46 Hz IMC during recovery in Monkey Be (**E**) and Monkey Mu (**F**). **a**: Coupling between ED23 and a variety of other muscles (see inset). **b**: Coupling between ADP and a variety of other muscles (see inset). n.s. in **a** and **b** indicates coherence values that were not significant. The gray horizontal lines in **a** and **b** represent the 95% confidence limit of coherence. Abbreviations; ADP: *adductor pollicis*, FDI: *first dorsal interosseus*, EDC: *extensor digitorum communis*, ED23: *extensor digitorum 2 and 3*, ED45: *extensor digitorum 4 and 5*, FDS: *flexor digitorum superficialis*, FCR: *flexor carpi radialis*, FCU: *flexor carpi ulnaris*, PL: *palmaris longus*, ECU: *extensor carpi ulnaris*, BB: *biceps brachii*

Figure 6. Schematic illustrations of the possible mechanisms underlying functional recovery after the l-CST lesion, proposed from the present results. **A**: In the intact state,

a direct CM connection (black) or peripheral feedback (green) contributes to generate the cortico-muscular coupling at the frequency of the β–band. **B**: During the recovery from l-CST lesion, subcortical neural systems (red) that mediate cortical command or peripheral feedback (green) to motoneurons might be involved in generating the 30-46 Hz IMC that emerged in a variety of hand/arm muscles. Dotted lines indicate polysynaptic connection.

Figure 1

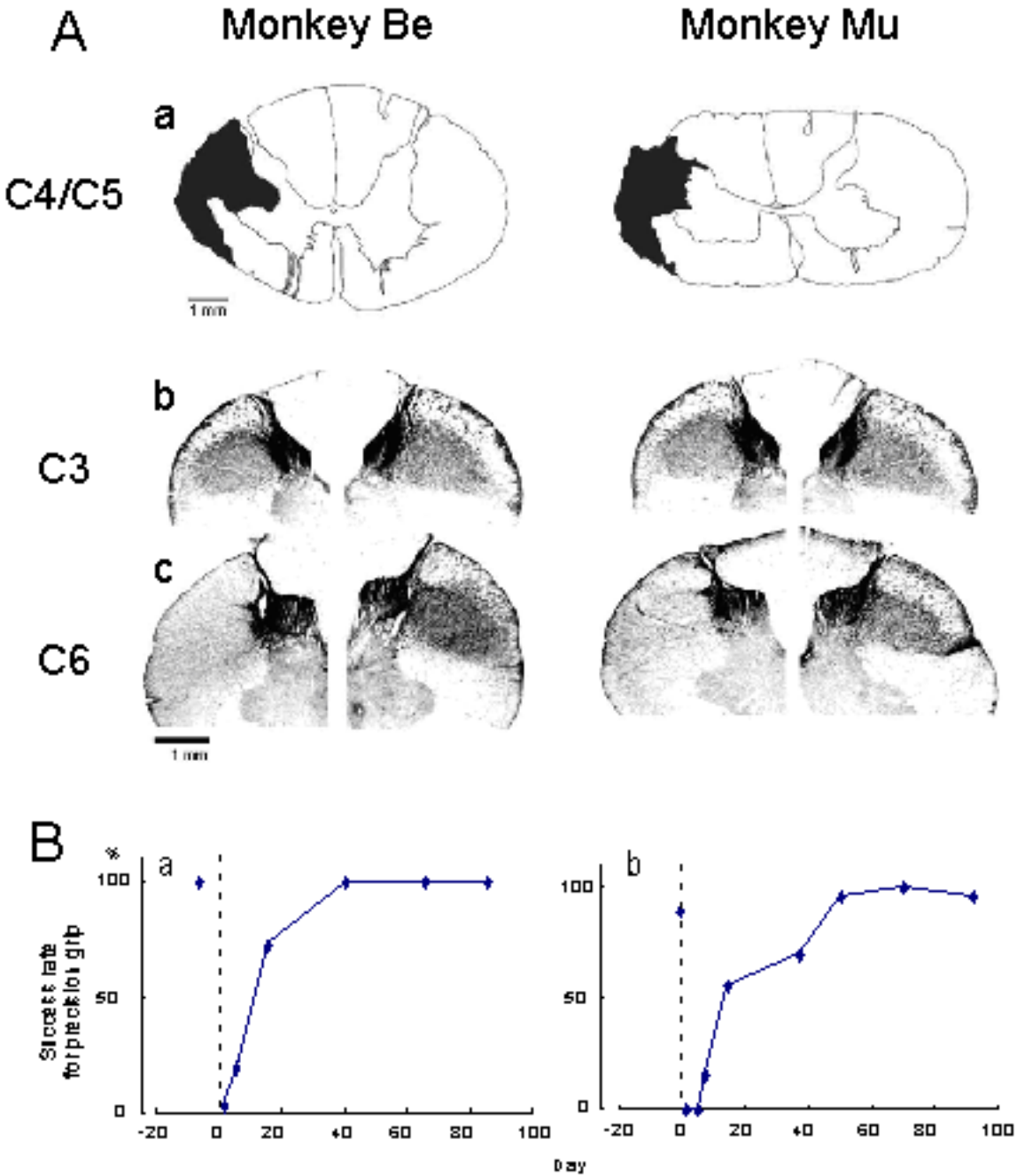
A
Monkey Be
Monkey Mu
a
C4/C5
1 mm
b
C3
c
C6
1 mm
B
a
b
%
100
50
0
-20
0
20
40
60
80
100
Day

Figure 2

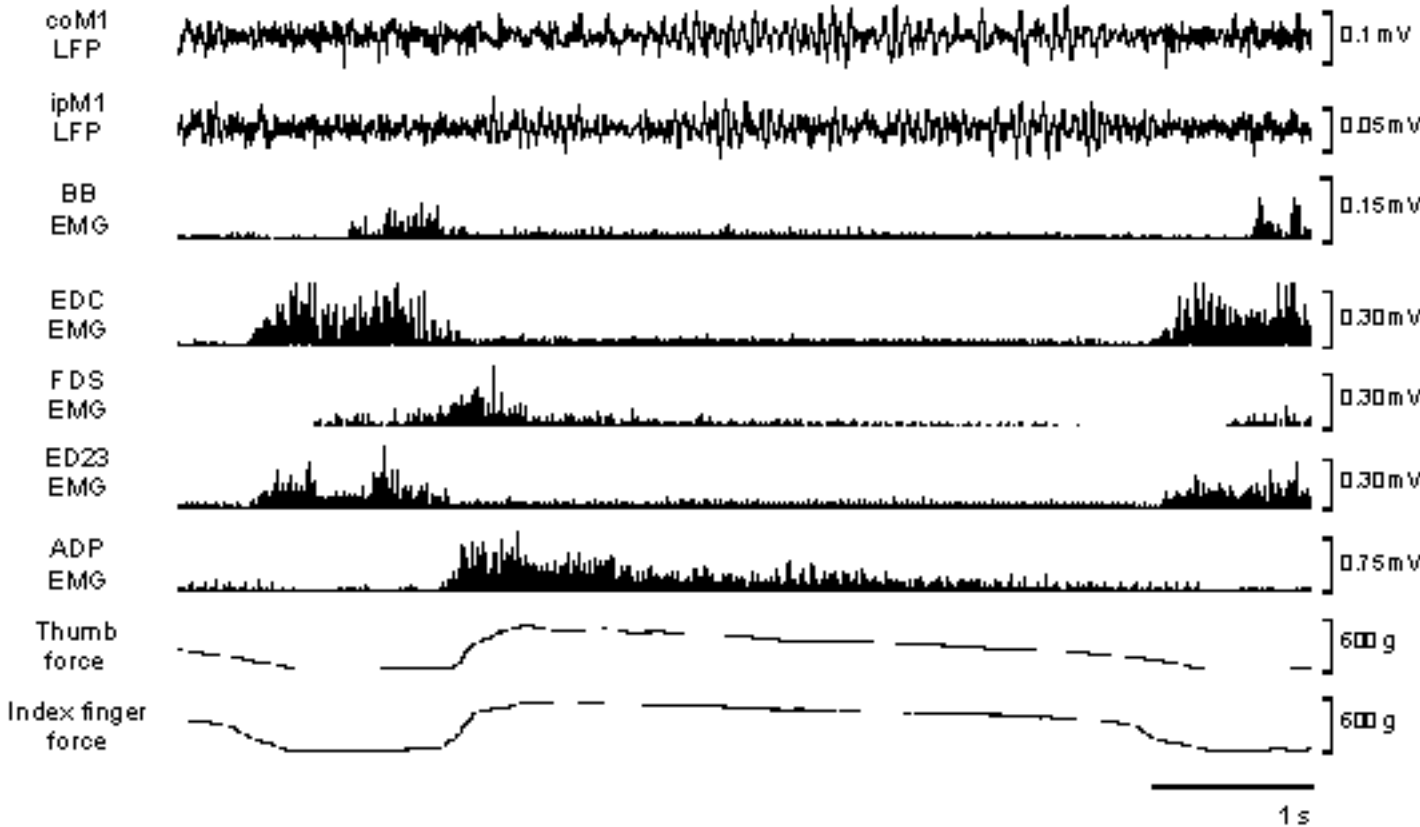
coM1
LFP
0.1 mV
ipM1
LFP
0.05 mV
BB
EMG
0.15 mV
EDC
EMG
0.30 mV
FDS
EMG
0.30 mV
ED23
EMG
0.30 mV
ADP
EMG
0.75 mV
Thumb
force
600 g
Index finger
force
600 g
1 s

Figure 3

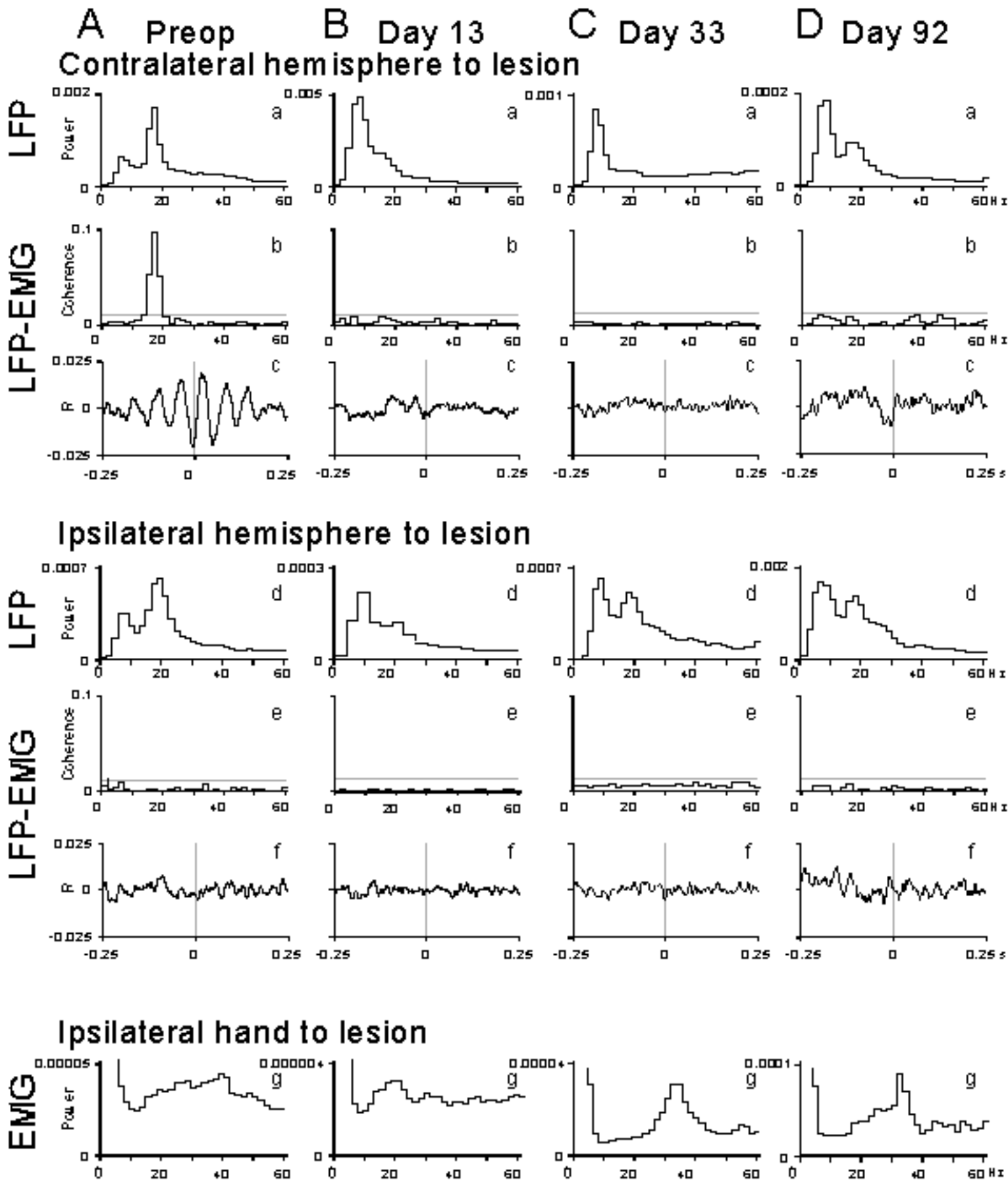
A Preop
B Day 13
C Day 33
D Day 92
Contralateral hemisphere to lesion
LFP
LFP-EMG
Power
Coherence
R
Ipsilateral hemisphere to lesion
LFP
LFP-EMG
Power
Coherence
R
Ipsilateral hand to lesion
EMG
Power
Hz
s

Figure 4

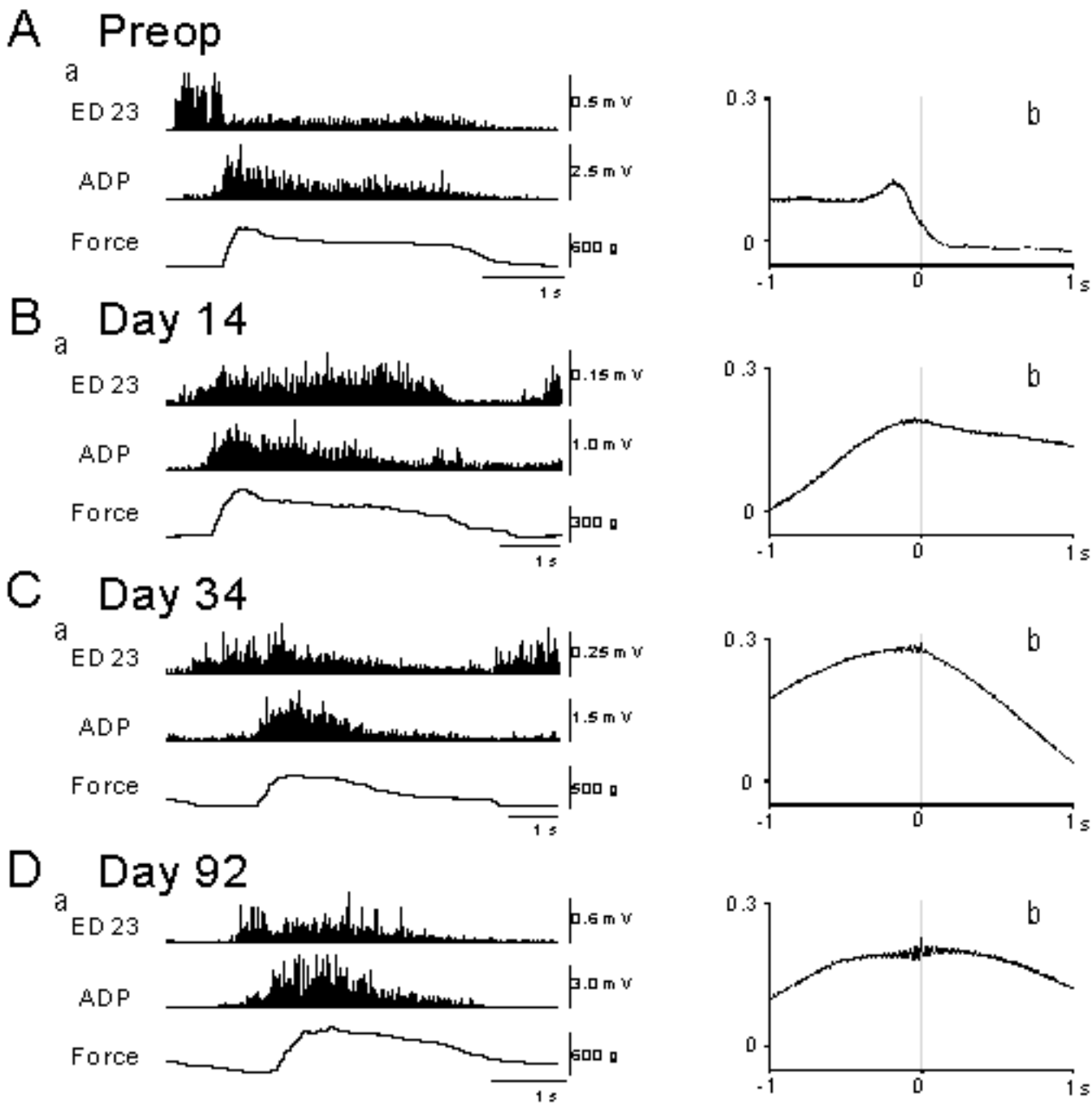
A Preop
a
ED23
ADP
Force
0.5 mV
2.5 mV
500 g
1 s
b
0.3
0
-1
0
1 s
B Day 14
a
ED23
ADP
Force
0.15 mV
1.0 mV
300 g
1 s
b
0.3
0
-1
0
1 s
C Day 34
a
ED23
ADP
Force
0.25 mV
1.5 mV
500 g
1 s
b
0.3
0
-1
0
1 s
D Day 92
a
ED23
ADP
Force
0.6 mV
3.0 mV
500 g
1 s
b
0.3
0
-1
0
1 s

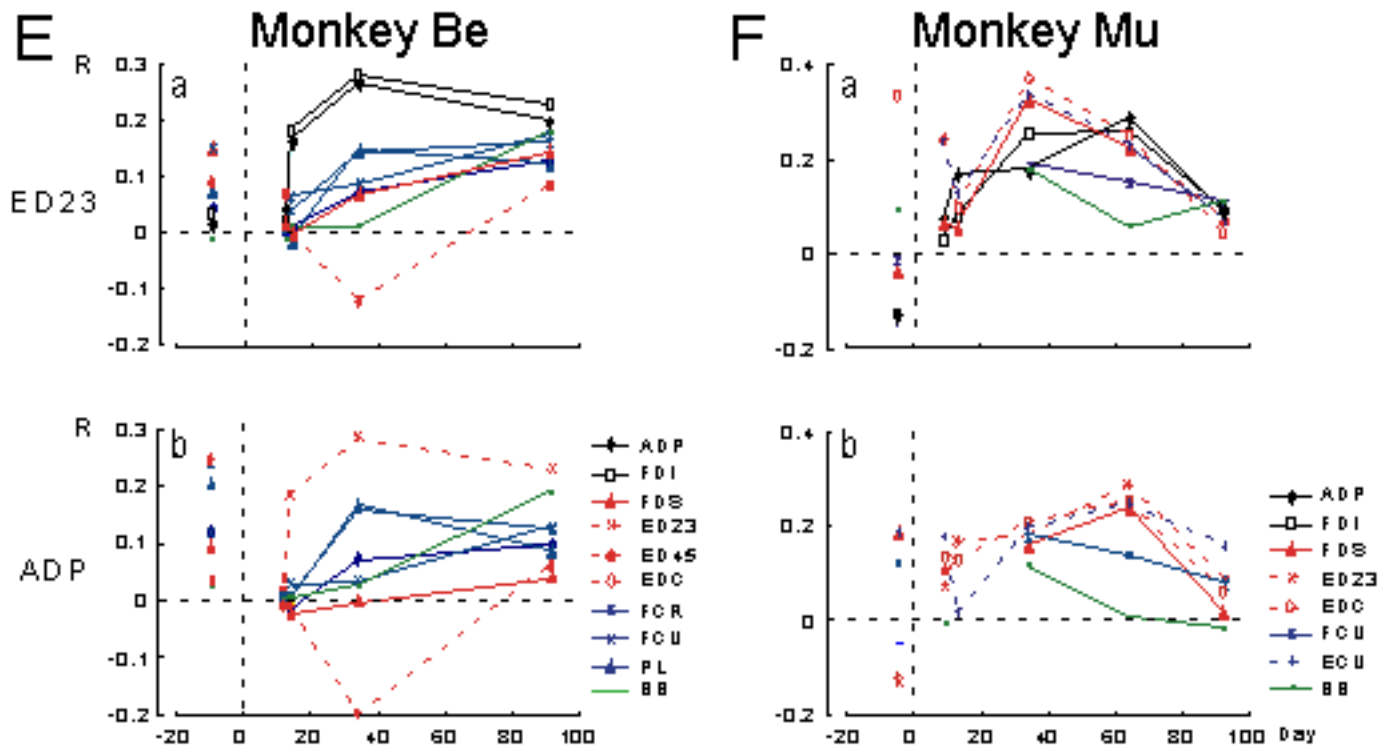
E Monkey Be
R
a
ED23
0.3
0.2
0.1
0
-0.1
-0.2
b
ADP
ADP
FDI
FDS
ED23
ED45
EDC
FCR
FCU
PL
BB
-20
0
20
40
60
80
100
F Monkey Mu
a
0.4
0.2
0
-0.2
b
ADP
FDI
FDS
ED23
EDC
FCU
ECU
BB
Day

Figure 5

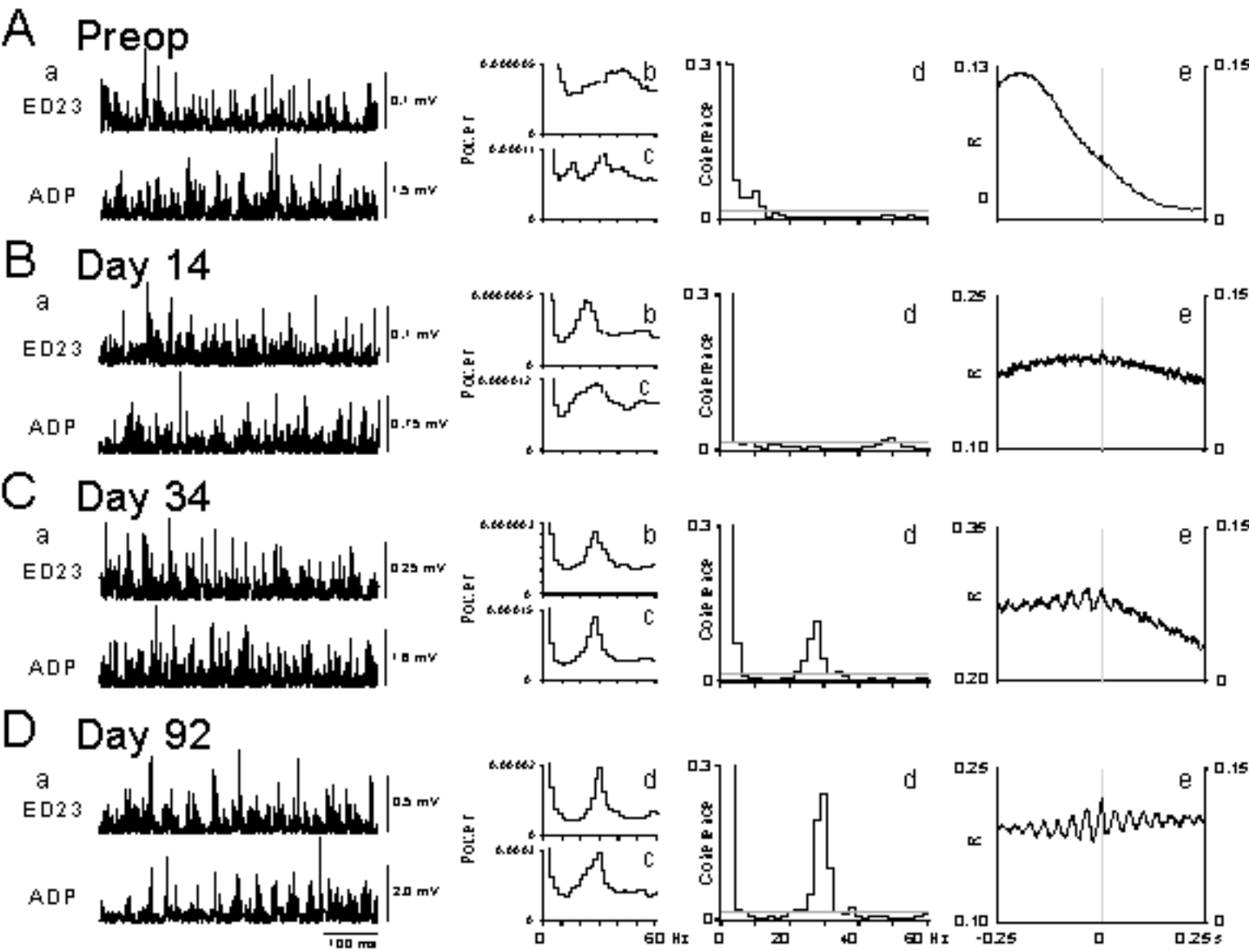
A Preop
B Day 14
C Day 34
D Day 92
a
ED23
ADP
b
c
d
e
Pol.Pr
Coherence
R
60 Hz
100 ms

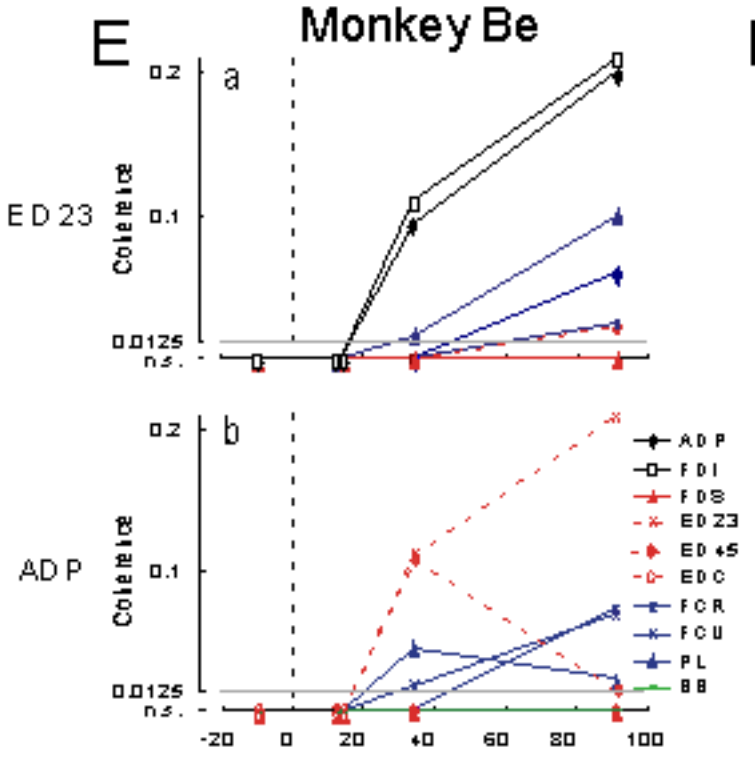
E
Monkey Be
F
Monkey Mu
a
b
ED23
ADP
Coherence
n.s.
ADP
FDI
FDS
ED23
ED45
EDC
FCR
FCU
PL
BB
ECU
Day

Figure 6

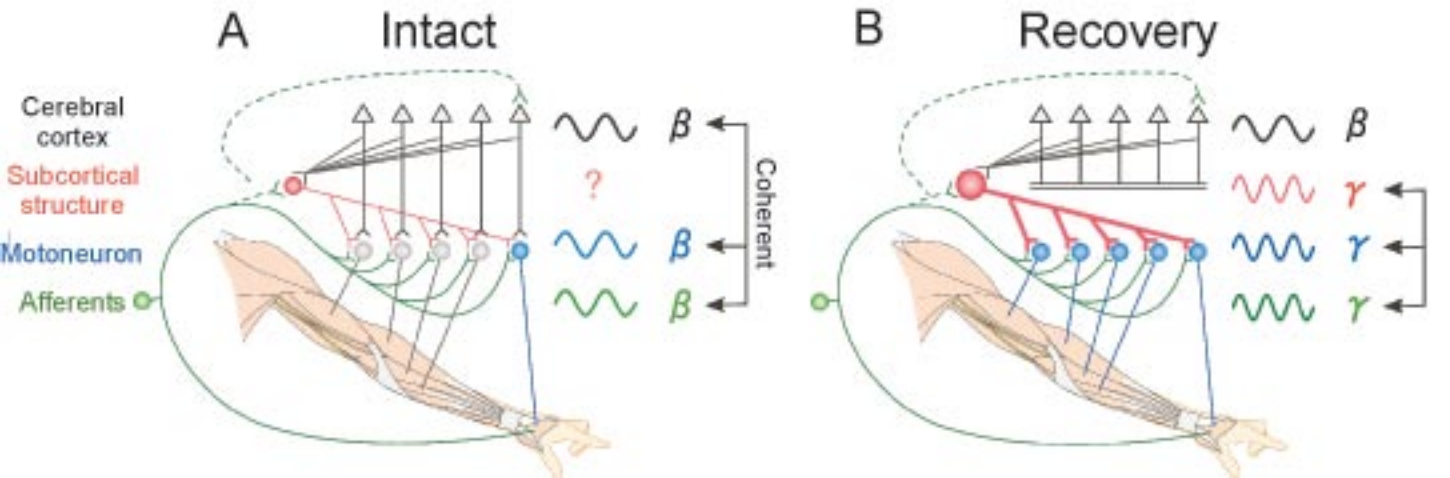
A
Intact
B
Recovery
Cerebral cortex
Subcortical structure
Motoneuron
Afferents
β
?
β
β
Coherent
β
γ
γ
γ